Ser. Cient. INACH 35: 39-63, 1986

# Thermal Structure and Heat Fluxes at Bransfield Strait during SIBEX 1985 (SIBEX-Phase II, Chile)

RICARDO ROJAS R.[1]

*ABSTRACT*

*During the austral summer of 1985 the second phase of SIBEX (Second International BIOMASS Experiment) took place. Chile, through the Instituto Antártico Chileno (INACH), participated in this phase, during which a cruise named SIBEX-Phase II performed oceanographic observations in the Bransfield Strait, between January 20th and February 15th, 1985.*

*The Instituto Hidrográfico de la Armada (IHA) continued the study of the thermal structure of the Bransfield Strait, which was initiated during SIBEX-Phase I. A total of 57 XBT and salinity samples were obtained. Using the meteorological data of the area a heat flux budget was made.*

*The temperature distribution pattern of SIBEX-Phase I, was similar to that of SIBEX-Phase II though higher temperatures were found in the northern portion of the strait during the last cruise. Except for the level at 50 m depth, the temperatures between the two cruises were statistically not different (99% confidence).*

*From the surface temperature, salinity and density distributions it was not evident the presence either of the formation of the meander between Deception and Brabant Islands or the Weddell Scotia Confluence south of Elephant and Clarence Islands. A cyclonic eddy located south of King George Island is suggested by the surface isopicnal distribution.*

*Regarding the heat flux budget in the Bransfield Strait an atmosphere to ocean heat transfer of 222 ± 83.4 (cal/cm$^2$ day) was obtained which agrees with heat flux estimates for the same period for the Southern Ocean (Gordon, 1981). Using a simple box model for the area, the rate of heat flux to the waters of the strait between atmosphere and advective processes is 2:1.*

*RESUMEN*

*Durante el verano austral de 1985 se realizó la segunda fase del crucero SIBEX, una componente del Programa Internacional BIOMASS (Biological Investigations of Marine Antarctic Systems and Stocks). Chile participó en esta etapa a través del Instituto Antártico Chileno (INACH) con un crucero denominado SIBEX-Fase II a bordo de la M/N Capitán Luis Alcázar, realizando observaciones oceanográficas en el área del estrecho Bransfield, entre el 20 de enero y el 15 de febrero de 1985.*

*El Instituto Hidrográfico de la Armada (IHA) participó en este crucero continuando con el estudio de la estructura térmica del estrecho Bransfield iniciado en SIBEX-Fase I. Se realizaron un total de 57 observaciones con XBT y de salinidad superficial. Se utilizó la información meteorológica para realizar un balance de calor en el área.*

*Existe una gran similitud entre la distribución de temperatura de SIBEX-Fase I y SIBEX-Fase II aun cuando se encontraron mayores temperaturas al norte del estrecho durante este último crucero. Estadísticamente, los promedios de temperatura por niveles, entre ambos cruceros, son iguales al nivel de confianza del 99%, a excepción del nivel de profundidad de 50 m.*

*De la distribución superficial de temperatura, salinidad y densidad, no se evidenció claramente la confluencia Weddell-Scotia al sur de las islas Elefante y Clarence, ni la formación del meandro entre isla Decepción y Brabante. El anillo ciclónico, localizado al sur de isla Rey Jorge, queda sugerido por la distribución de isopicnas superficiales.*

*Respecto del balance de calor en el estrecho de Bransfield, se computó un flujo neto de calor de la atmósfera al océano del orden de 222 ± 83.4 (cal/cm$^2$/día) concordante con estimaciones para el mismo período en la región del Océano Austral (Gordon, 1981). Utilizando un simple modelo de caja en el área, se estimó que el aporte de calor a las aguas del estrecho, por parte de la atmósfera y de procesos advectivos, está en la proporción de 2:1.*

(1) Departamento de Oceanografía, Instituto Hidrográfico de la Armada, Casilla 324, Valparaíso, Chile.

## INTRODUCTION

The Bransfield Strait, located between the Antarctic Peninsula and the South Shetland Islands, has been a focus of attention by the scientific community during the last few years, largely as a result of the development of the BIOMASS program.

Previous studies (Clowes, 1934; Gordon and Nowlin, 1978) characterize the area as one having special bathymetric and oceanographic features. It is influenced mainly by the adjacent Bellingshausen Sea, to the southwest, and the Weddell Sea, to the southeast. The deep waters of the three basins, practically confined inside the strait, are renewed by local convection during the winter period (Clowes, 1934).

Chile has participated in the BIOMASS program, through oceanographic cruises coordinated by INACH during the austral summers of 1981 (FIBEX) and 1984 (SIBEX-Phase I). The physical-chemical results of those cruises have been presented by Sievers (1982), Salamanca and Acuña (1982), Kelly *et al.* (1985), Silva (1985) and Rojas (1985).

During the austral summer of 1985, INACH coordinated the second part of this program named SIBEX-Phase II. The cruise was performed from January 20th to February 15th, 1985 on board M/N Capitan Luis Alcazar.

The IHA participated in this second phase with a high density sampling in the area using XBT's, a continuation of the study initiated during the summer of 1984 (SIBEX-Phase I). The specific goals of this study are: a) to examine the temperature distribution in the Bransfield Strait during the summer of 1985, and compare it with that obtained during FIBEX and specially SIBEX-Phase I; b) to compare both phases of SIBEX regarding frontal zones and permanence of certain oceanographic features characteristic of the area; and c) to consider the contribution of the Bransfield Strait to the heat budget in the Southern Ocean during the period of observation. To do the latter, a computation of heat exchange between the atmosphere and the ocean is made. Also a simple heat balance for the area is analyzed.

## MATERIALS AND METHODS

Figure 1 shows the area covered during the second phase of SIBEX. Points in the figure correspond to locations where XBT observations were taken and water samples obtained for surface salinity analysis. T-7 (0-760 m) and T-4 (0-460 m) probes were used for the XBT sampling; a total of 57 records were obtained in the area.

The XBT records were read through computer programs using a digitizer. The surface salinity samples were analyzed at the IHA using an Autolab salinometer model 601.

### Temperature distribution

Horizontal temperature distributions were prepared at 0, 25, 50, 100, 200 and 300 meters levels. 13 sections with a general north-south direction and 2 sections along the axis of the strait were prepared to show vertical temperature distributions (Figure 1).

A statistical comparison of temperatures was made for both SIBEX-Phases I and II (Ostle and Mensing, 1979). This procedure was performed using temperature averages and variances at the different depth levels. The following tests were applied to the data:

Test of comparison of variances (F test) and test of comparison of the means (student-t test). Table 1 summarizes the hypothesis for each test at the confidence levels considered.

Table 1

TESTS USED TO COMPARE TEMPERATURE AT DEPTH LEVELS OF 0, 25, 50, 100, 200 AND 300 METERS FROM CRUISES SIBEX-PHASE I (JANUARY-FEBRUARY, 1984) AND SIBEX-PHASE II (JANUARY-FEBRUARY 1985). CONFIDENCE LEVELS CONSIDERED $\alpha = 0.05$ (95%) AND $\alpha = 0.01$ (99%)

| Test | Hypothesis | Test | Critical Region |
|---|---|---|---|
| Comparison of variances | H: $\sigma_1^2 = \sigma_2^2$<br>A: $\sigma_1^2 \neq \sigma_2^2$ | $F = \frac{S_1^2}{S_2^2}$ | $F < F_{\left(\frac{\alpha}{2}\right)(n_1-1,\ n_2-1)}$ |
| Comparison of means | H: $\mu_1 = \mu_2$<br>A: $\mu_1 \neq \mu_2$ | $t = \frac{\overline{X}_1 - \overline{X}_2}{\left(S^2\left(\frac{1}{n_1} + \frac{1}{n_2}\right)\right)^{1/2}}$ | $t \geq t_{\left(1-\frac{\alpha}{2}\right)(n_1+n_2-2)}$ |

$\mu$ and $\sigma^2$ are the mean and variance of each normal distribution. $\overline{X}$, $S^2$ and n are the mean, variance and number of observations of each finite sampling. The subscripts 1 and 2 identify SIBEX I and II cruises respectively.

**Heat balance at the sea surface**

During the cruise regular observations of air temperature, wind speed, surface salinity, atmospheric pressure and sea surface temperature were collected. Using these data, an estimate of heat transfer between ocean and atmosphere was computed for the Bransfield Strait area. The formulae are given in the following paragraphs.

The total heat flux at sea surface is composed of: $Q_S$ the incoming radiation from sun and sky; $Q_B$ the effective back radiation from the sea surface; $Q_E$ the heat used for evaporation and $Q_H$ the exchange of sensible heat between ocean and atmosphere.

These four components determine the total heat received or lost by the ocean at the sea surface, according to the relation:

$$Q_T = Q_S - Q_B - Q_E - Q_H \quad (1)$$

The direct and diffuse solar radiation $Q_S$ that is absorbed by the water is:

$$Q_S = Q_{SO}\ (1 - 0.62 * N + 0.0019 * A) \quad (2)$$

where $Q_{SO}$ is radiation at cloudless sky conditions (function of latitude and month). They are obtained from the Smithsonian Meteorological Tables (List, 1951); N is the cloud cover factor in tenths and A is the noon sun altitude in degrees.

The effective back radiation Q is given by:

$$Q_B = (e\ s\ Ts\ (0.39\text{-}0.05\ f^{\frac{1}{2}}) + 4\ e\ s\ Ts\ (Ts\text{-}Ta)\ (1\text{-}0.7\ N) \quad (3)$$

where e = 0.97 is the emissivity of the sea surface; s = 5.673 x $10^{-8}$ W $m^{-2}$ $K^{-4}$ is the Stefan-Boltzmann constant; f = is the vapor pressure of the air in mb; Ts = is the sea surface temperature in °K and Ta = is the temperature of the air in °K.

The formulae to compute heat used for evaporation and sensible heat flux are respectively

$$Q_E = @C_E\ L_E\ (qs - qa)\ U \quad (4)$$
$$Q_H = @c_p\ WT \quad (5)$$

where @ is air density; $C_E$ is the evaporation coefficient; $L_E$ is the latent heat of evaporation; qs is the saturation specific humidity of air at the temperature of the sea surface; qa is the specific humidity of the air; U is wind velocity; c is the heat capacity for dry air and WT is the vertical turbulent flux temperature in the atmosphere, which is given by:

$$1.69 \times 10^{-3} + 0.82 \times 10^{-3}\ U\ (Ts\text{-}Ta) \quad \text{for } (Ts\text{-}Ta) < 0 \quad (6a)$$
$$2.24 \times 10^{-3} + 1.12 \times 10^{-3}\ U\ (Ts\text{-}Ta) \quad \text{for } (Ts\text{-}Ta) > 0 \quad (6b)$$

Equations 6a and 6b have been suggested by Anderson and Smith (1981) for a stable and unstable atmosphere respectively.

The heat flux estimates for the period of observation contain spatial and temporal variations which need to be minimized. For this analysis, in situ values were averaged on a 0.5 latitude by 1 longitude grid. Anomalies were then computed by substracting from each value the monthly average of the parameter. Due to the short duration of the cruise and the restricted area considered, a value of 5 tenths in cloud cover was used in the corresponding formulas. This is equivalent to considering partial cloudiness during the whole cruise.

## RESULTS

### Levels and sections

The temperatures found in the area range between approximately -1.0 °C (300 m), southeast of the strait, and over 2.0 °C in the northern surface portion, south of the South Shetland Islands.

The surface temperature distribution from SIBEX-Phase II is shown in Figure 2.a. A strong meridional temperature gradient is observed in the central and eastern part of the strait. A similar gradient, but not so strong, was observed during SIBEX-Phase I.

At levels 25 and 50 m the same temperature distribution of the surface holds, even though the temperature gradient mentioned above decreased with depth (Figure 3.a). In these three levels the waters of the strait are dominated by positive temperatures.

At the three remaining levels (100, 200 and 300 m), the opposite picture is found, i.e. the strait is dominated by negative temperatures. At depth, the isotherms tend to follow the configuration of the axes of the central and western basins, located southward of the South Shetland Islands (Figure 4a).

In Figures 2b to 4b the position of a pair of isotherms from SIBEX-Phases I and II are shown for each respective level. There is a predominance of warmer waters at levels 0, 25 and 50 m in SIBEX-Phase II as compared to SIBEX-Phase I. This is shown by the southward displacement of the 1.5 °C isotherm in SIBEX-Phase II in each figure. This isotherm is even found at the 100 m level (Figure 4b) in this last cruise.

At levels 100, 200 and 300 m the position of the two isotherms during both cruises are quite similar, illustrating the importance of the cold water advection from the Weddell Sea with respect to the warmer waters advected from the north. The position of the 0 °C isotherm in both cruises is nearly coincident at every depth. This isotherm is found near the Antarctic Peninsula shelf at shallow depths and at the axes of the basins at deeper levels.

The vertical distribution of temperature was plotted in 13 sections perpendicular to the strait and in 2 parallel sections. Only some of them are presented in this study.

The penetration of cold waters coming from the Weddell Sea can be observed in sections 1 to 3, which are advected into the strait through the Antarctic Sound and eastward D'Urville Island. These cold waters deeppen as they move northwards, filling the central and eastern basins of the strait (Figures 5 and 6).

This distribution is similar to the one found during 1984 with the exception that, in the northern part of the strait, the positive isotherms are deeper in SIBEX-Phase II than in SIBEX-Phase I, showing a major intrusion of warmer waters into the strait.

This pattern can also be observed in the central part of the strait in sections C to 5, i.e. the contrast between the warm surface waters found at the northern part of the strait and the cold deeper waters from the Antarctic Peninsula shelf and the central basin. Again positive isotherms at the northern part of the strait are deeper in SIBEX-Phase II than in SIBEX-Phase I (Figures 7 and 8).

The same situation is observed in the last sections of SIBEX-Phase II (sections E to 7). Warm waters coming from the Bellingshausen Sea and the Gerlache Strait limit the northward and westward extension of the cold Weddell Sea waters over the shelf of the Antarctic Peninsula (Figures 9 and 10).

Finally, the longitudinal sections 8 and 9 (Figures 11 and 12) from SIBEX-Phase II show the same panorama from SIBEX-Phase I, i.e. the zonal influence of the cold waters from the Antarctic Peninsula shelf at the Bransfield Strait, which extends further westwards on the southernmost section (section 9, Figure 12).

**Statistical comparison**

Temperature data from SIBEX-Phase I and SIBEX-Phase II were compared by using test of variances and means. Figure 13 shows the temperature averages at different levels (0, 25, 50, 100, 200 and 300 meters) for both cruises. Confidence levels for 95% and 99% are also included in the figure as well as the corresponding values from FIBEX which were discussed by Rojas (1985) as part of the analysis of SIBEX-Phase I.

At every compared depth, the variances from the means on both cruises proved to be the same at the 99% confidence level.

Regarding the temperature means, at every compared depth and at the 95% confidence level, the temperature averages from both cruises were different. However, at the 99% confidence level all the temperatures averages proved to be not statistically different, with the only exception being the 50 m depth level.

### Heat fluxes

Figures 14 to 17 show the horizontal distribution of the fluxes considered in equation 1. All fluxes are expressed in (cal/cm$^2$/day) units. The figure corresponding to the Qs component has not been included since this component varies slightly with the season, and even less regionally.

The total heat flux distribution is shown in Figure 14. There is a net heat flux from the atmosphere to the ocean all over the strait, with maximum values south of Elephant, Smith and Snow Islands. Minimum values are found at the central part of the strait and also at the easternmost portion of the Gerlache Strait.

Values of sensible heat flux and heat used for evaporation, shown in Figures 16 and 17, were mainly negative, illustrating the loss of heat from the atmosphere to the ocean. This is due to the positive difference between the air temperature (Ta) and the sea surface temperature (Ts) found over most of the strait during the cruise. Distributions of both fluxes are very much alike, with larger values in heat flux used for evaporation. Both distributions show maximum values in the northeastern and northwestern portion of the strait as a result of the higher wind speeds found on those relatively open areas. Values of sensible and heat used for evaporation from the ocean to the atmosphere were found at the central portion of the strait as a result of the negative difference between Ta and Ts. This difference produced the maximum values in longwave back radiation emitted from the ocean to the atmosphere (Figure 25).

Figures 18 to 20 show the total, sensible and heat used for evaporation components on which the respective mean value for the area during the cruise have been removed. Therefore, these fluxes represent heat flux anomalies respective to the corresponding monthly signals.

The monthly variation of the net heat flux is shown in Figure 18. It is observed that during the cruise, the strait gained heat in its northeastern part and lost heat in its central and western portions. This is observed in the sensible and heat used for evaporation anomalies (Figures 19 and 20) for those portions of the strait.

It can be noted that the minimum values of net heat flux, south of King George Island (Figure 14), coincide with the maximum values of heat transfer once the monthly signal have been eliminated (Figure 18).

## DISCUSSION

During January-February, 1985 (SIBEX-Phase II), it was possible to repeat most of the XBT sections performed during the same months of 1984, except for those sections located westward of Anvers Island. However, more sections were made in SIBEX-Phase II than in SIBEX-Phase I, resulting in a better spatial resolution of temperature.

From a qualitative viewpoint, the horizontal and vertical temperature distributions from both cruises show small differences. In general, there was a larger advection of warm waters into the strait during SIBEX-Phase II. This is observed south of the South Shetland Islands in the upper 50 meters depth at the corresponding temperature levels and sections. Northward of the Antarctic Peninsula and mostly below 100 m all over the strait, the advection and influence of the cold waters from the Weddell Sea, arbitraryly defined by the 0 °C isotherm, is remarkably similar in both cruises.

Intrusions of surface waters of less salinity into the western region of the strait, as well as the lack of strong salinity gradients in its eastern portion during SIBEX-Phase II (Figure 21), highlight the difference in this parameter between the cruises. The resulting isopycnal distribution from SIBEX-Phase II (Figure 22) does not show clearly the formation of the meander between Deception and Brabant Islands, which has been previously reported (Clowes, 1934; Stein and Rakusa-Suszczewski, 1983; Guzman *et al*, 1983; Rojas, 1985). Besides the existence of the cyclonic eddy south of King George Island, also reported by the same authors, is suggested by the meander formed by the 27.4 isopycnal in that area. On the other hand, the isopycnal distribution does not clearly show the Weddell-Scotia confluence, which does not show a characteristic surface signal in temperature (Patterson and Sievers, 1982). Probably the intrusion of warm and less saline waters tends to mask its identification at the surface level.

The relative confinement of the Bransfield Strait gives us an idea regarding the spatial scales by which mixing and interaction processes occur, but not the temporal scales by which they take place. The statistical comparison between SIBEX-Phase I and SIBEX-Phase II, through temperature means by depth levels, allow us to observe the annual variability by comparing the vertical variability in temperature for cruises made during the same season of the year.

At the 95% confidence level the temperature averages for both cruises proved to be different at every depth. At a higher confidence level (99%) all the temperature averages proved to be equal with the exception of the 50 meter depth level. This exception could be due to the larger deepening of the positive isotherms found at the northern portion of the strait. In Figure 3b the 1.5 °C isotherm shows up at the northern part of the strait. That isotherm does not appear at that depth in SIBEX-Phase I. Therefore, higher temperatures in SIBEX-Phase II at the 50 meter depth level would make the respective temperature averages to be different between both cruises.

From the temperature distributions, as well as the results of the statistical tests one can conclude, in a general sense, that the temperature averages for both SIBEX-Phase I and SIBEX-Phase II were quite similar among them, contrasting with those from FIBEX, whose temperatures were statistically lower (Rojas, 1985).

Regarding the heat balance for the Bransfield Strait area, the heat flux components showed a relatively large variability on their corresponding horizontal distributions. The only region in which heat fluxes from the ocean to the atmosphere were obtained, corresponded to the place where the cyclonic eddy was located. That can be explained because of the longer residence time of warm waters in that area, as a result of the cyclonic eddy, could eventually allow an ocean to atmosphere heat transference.

In spite of the variability on the heat exchange estimates, a net atmosphere to ocean heat flux was obtained during the period of the observation (January-February) for that

Bransfield Strait area. Averaging all the values of SIBEX-Phase II, a net heat flux of 222 $\pm$ 83.4 (cal/cm$^2$/day) from the atmosphere to the ocean is obtained. This excess of heat is important, because it is necessary to initiate and hold the dilution of marine and glacial ice during the austral summer. Gordon (1981) estimated heat surpluses of about 132 and 56 (cal/cm$^2$/day) for the months of January and February over a latitude band between 60 and 70 degrees in the Southern Ocean. The heat estimate from SIBEX-Phase II is similar to the estimates by Gordon (1981), however, that obtained here is larger.

If we consider a simple box model for the heat budget at the Bransfield Strait (Figure 23) in which we neglect the diffusive and convective changes, we can write:

$$Qa = Qt + Qv$$

where Qa is the change of heat contents ($\Delta$H) in the area per unit time, Qt is the net atmosphere-ocean heat flux and Qv is the heat introduced or took out from the area by advective processes. Formulas are included in Figure 23. XBT profiles obtained during SIBEX-Phase II allow us to compute the heat gained or lost during that period; therefore we can estimate the advective heat flux as a residual form.

The heat contents relative to 0° C was computed between the surface and 200 m depth, because this is the layer on which temperature changes occur. Comparisons of XBT profiles from SIBEX-Phase I and Phase II for common geographical areas show that deeper than 200 m the XBT profiles become equal. Figure 24 shows the values of H for each one of the sections considered. It can be observed that the values of $\Delta$H tends to decrease and become negative in the south.

Averaging all the values obtained during the period of observation, a value of 376 $\pm$ 663 (cal/cm$^2$/day) was obtained for the volume considered. In spite of the large variability in this estimation we can use it to obtain the advective flux as a residual term, which happens to be 154 $\pm$ 657 (cal/cm$^2$/day). Therefore, using this simple box model we can state that the ratio of heat supplied to the waters of the strait between atmosphere and advective processes is 2 to 1.

Finally a word of caution. We have to keep in mind that the heat flux estimates computed in this study are exposed to errors, either by using meteorological formulas which use empirical constants or biased by sampling problems (synopticity) which are inherent to these sorts of measurements. Nevertheless, these values represent an independent estimate of the net heat flux at the Bransfield Strait area during the summer of 1985.

## CONCLUSIONS

The temperature distribution during SIBEX-Phase II es quite similar to the one found during SIBEX-Phase I. The main difference is found at the northern part of the strait where higher temperatures, between surface and 50 m depth, were found during SIBEX-Phase II. At other depths in the strait the temperature distribution remained almost unchanged from one cruise to the other.

From a quantitative statistical viewpoint, the temperature averages by depth levels from SIBEX-Phase II differ from those from SIBEX-Phase I at the 95% confidence level. At a better estimation level (99%) the averages from both cruises are the same, with

exception of the 50 m depth level. This similarity between these two consecutive cruises tends to show that the temperatures found during FIBEX in summer 1981 were anomalous.

From surface distributions of temperature, salinity and density the meander between Deception and Brabant Islands found in previous cruises was not clearly observed. The cyclonic eddy, previously observed south of King George Island, is suggested from the surface density distribution and the low values in the atmosphere-ocean heat flux in that area. The Weddell-Scotia confluence, commonly observed south of Clarence and Elephant Islands was not clearly observed during SIBEX-Phase II.

From the heat balance study in the Bransfield Strait, a net atmosphere to ocean heat flux of about $222 \pm 83.4$ (cal/cm$^2$/day) was found. This value is higher than Gordon's estimates (1981) of heat fluxes for the summer months at this Southern Ocean latitude.

From the application of a simple heat balance box model for the Bransfield Strait, the contribution of the advective processes between surface and 200 m was obtained as a residual term. The ratio of heat supplied to the waters of the strait from the atmosphere and advective processes was computed to be 2:1.

## ACKNOWLEDGEMENT

The author wishes to express his gratefulness to the Instituto Antartico Chileno by affording this current study and to the Captain and crew members of M/N Capitan Luis Alcazar by their altruistic collaboration during the cruise.

He also wishes to thank the people of the IHA Oceanography Department who participated in data processing and reduction, especially Mr. E. Aravena, Ch. Bonert, L. Toro, A. Sanchez and Miss R. Dorion.

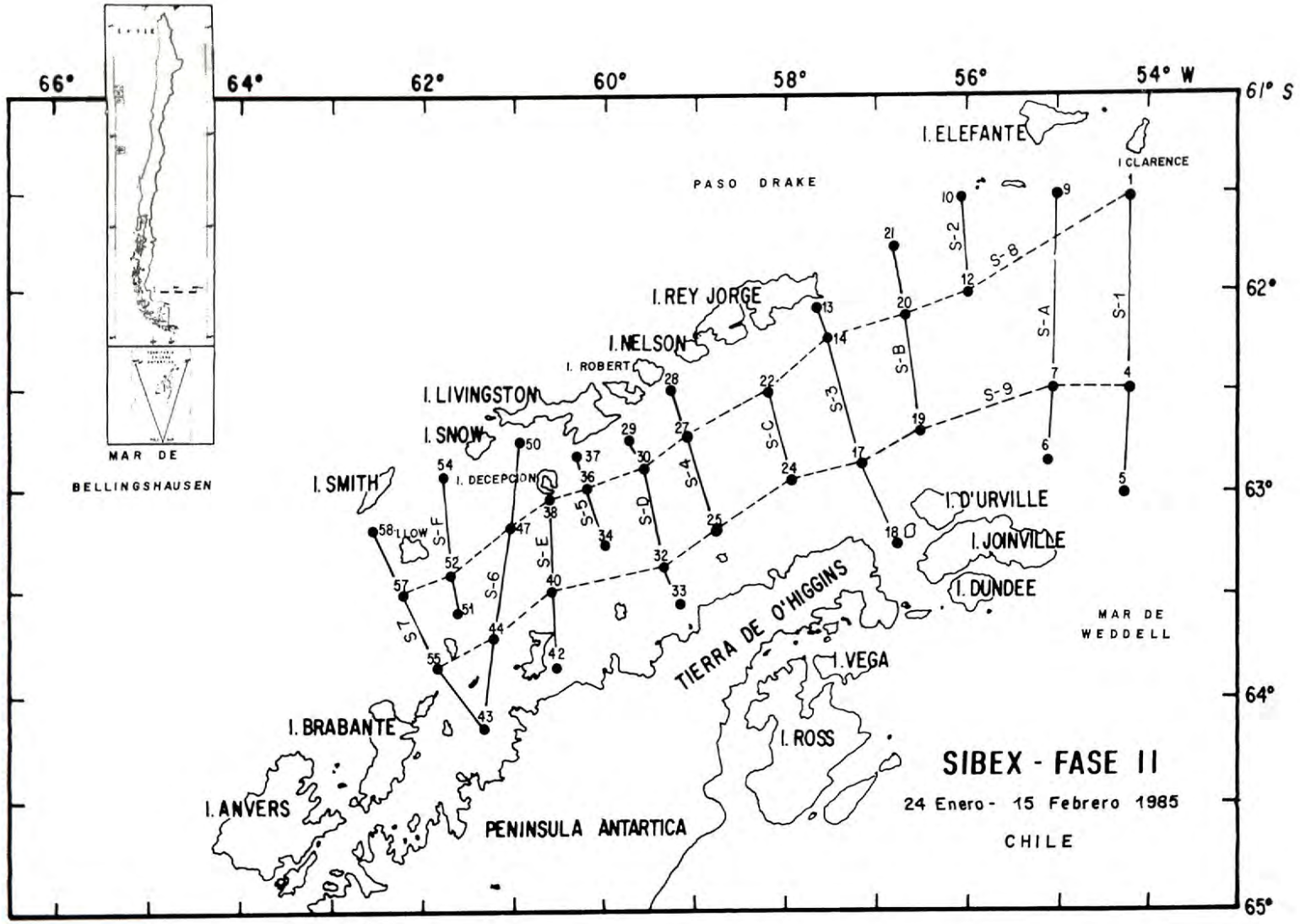


Figure 1.—Geographic position of the observations and distribution of sections during SIBEX-Phase II (January 24 - February 15, 1985).

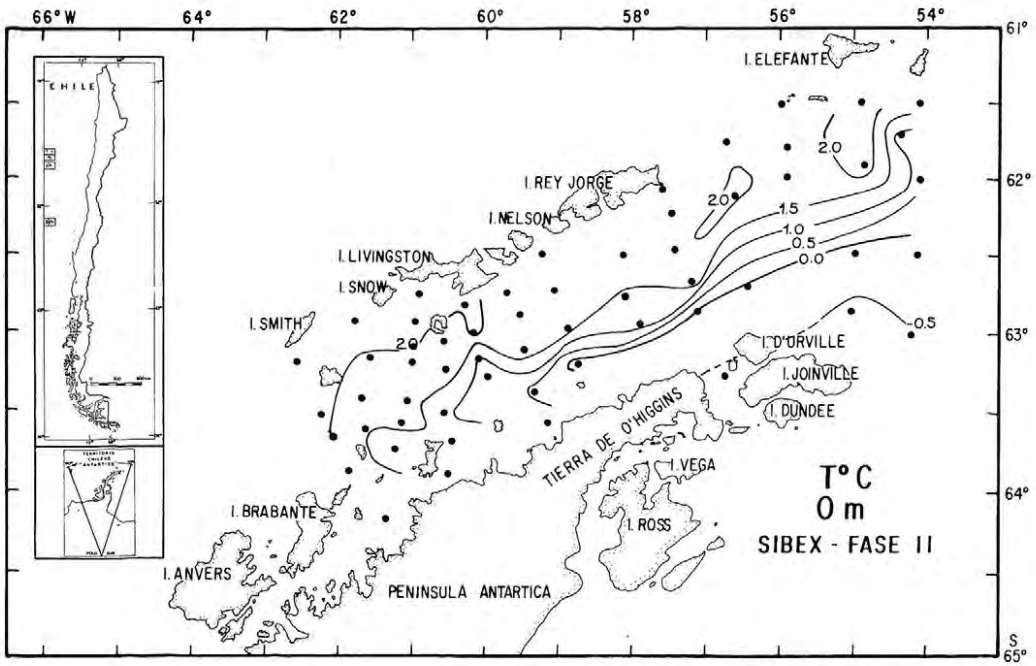


**Figure 2a.**—Horizontal distribution of temperature at 0 m level.

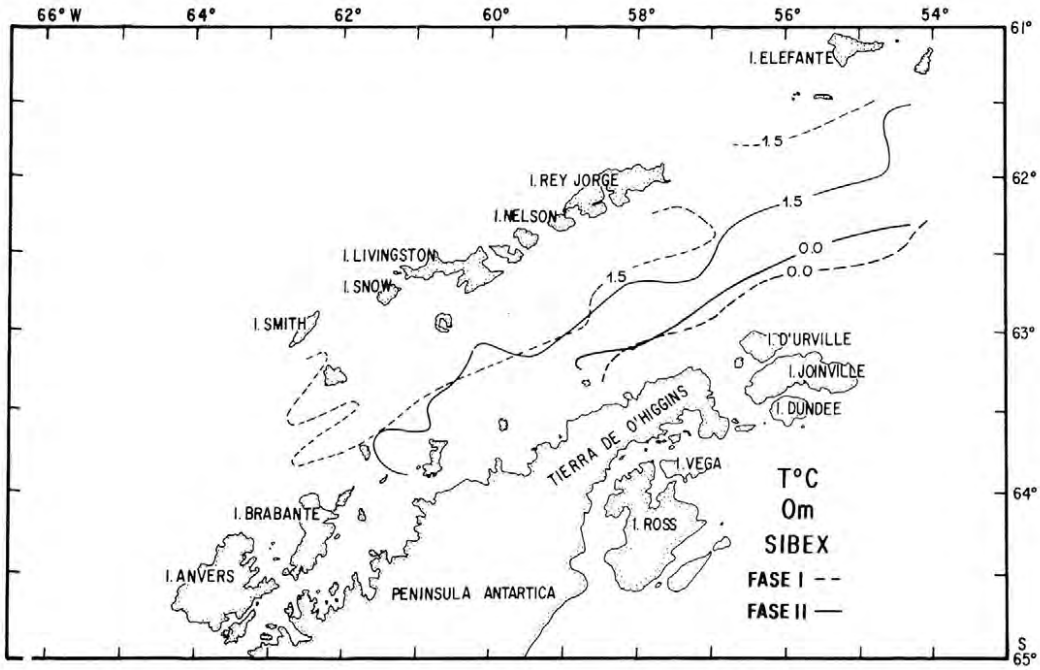


**Figure 2b.**—Position of a pair of isotherms of the SIBEX-Phase I (January 27 - February 10, 1984) and SIBEX-Phase II (January 24 - February 15, 1985) cruises at 0 m level.

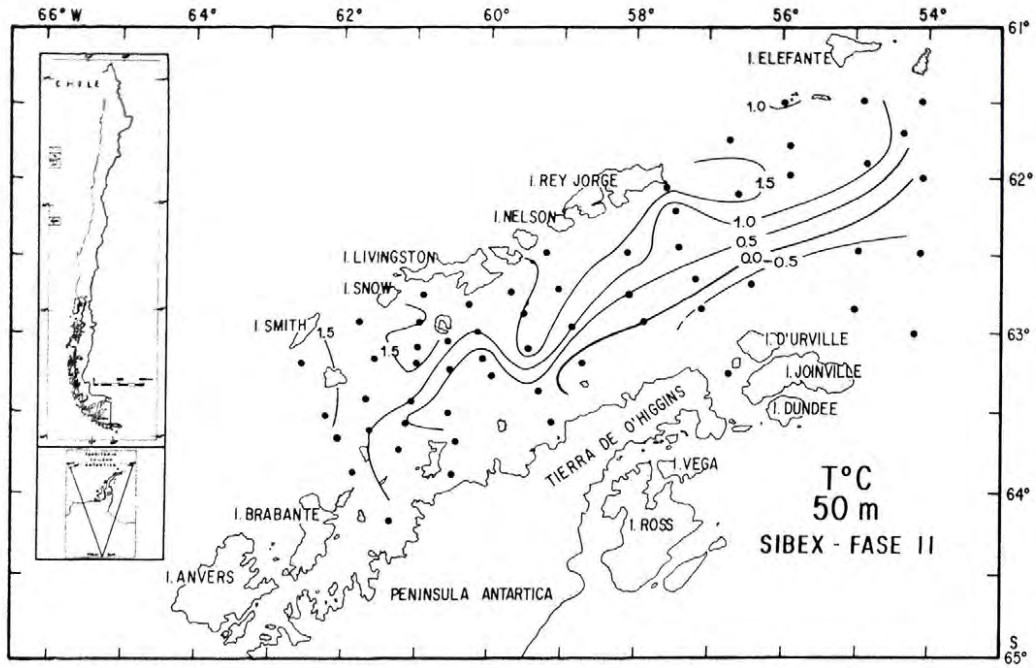


Figure 3a.—Horizontal distribution of temperature at 50 m level.

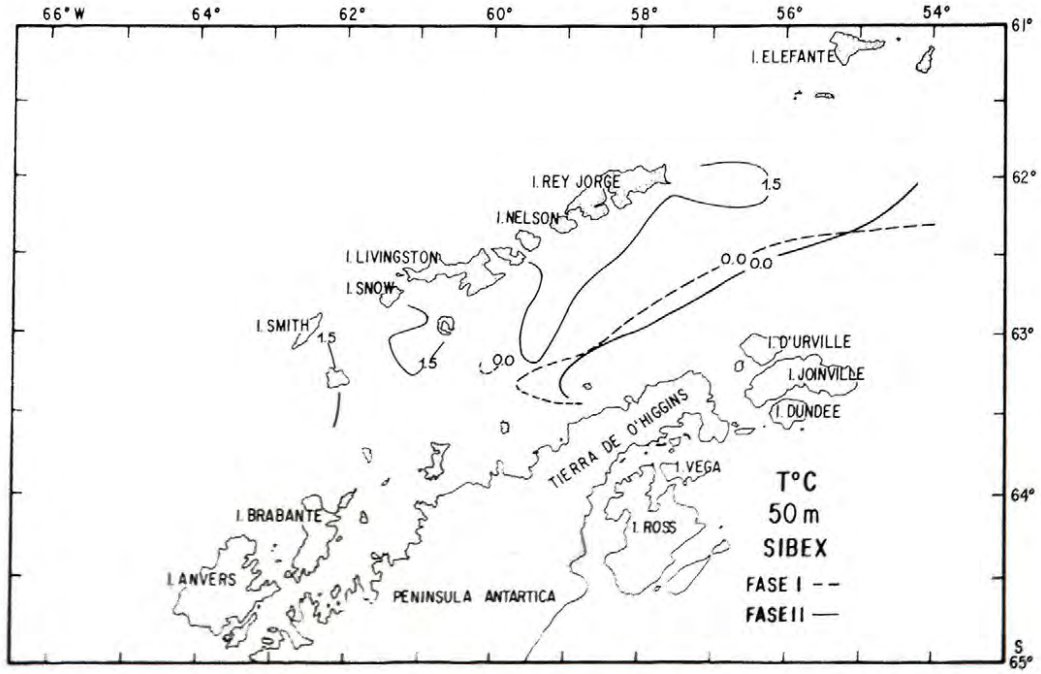


Figure 3b.—Position of a pair of isotherms of the SIBEX-Phase I (January 27 - February 10, 1984) and SIBEX-Phase II (January 24 - February 15, 1985) cruises at 50 m level.

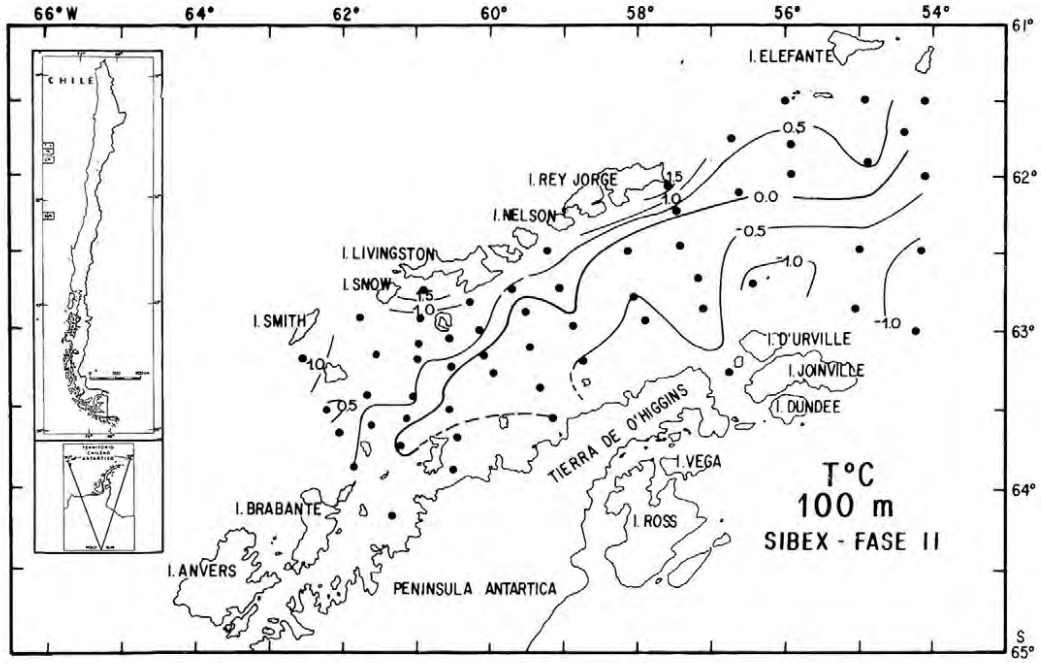


**Figure 4a.**—Horizontal distribution of temperature at 100 m level.

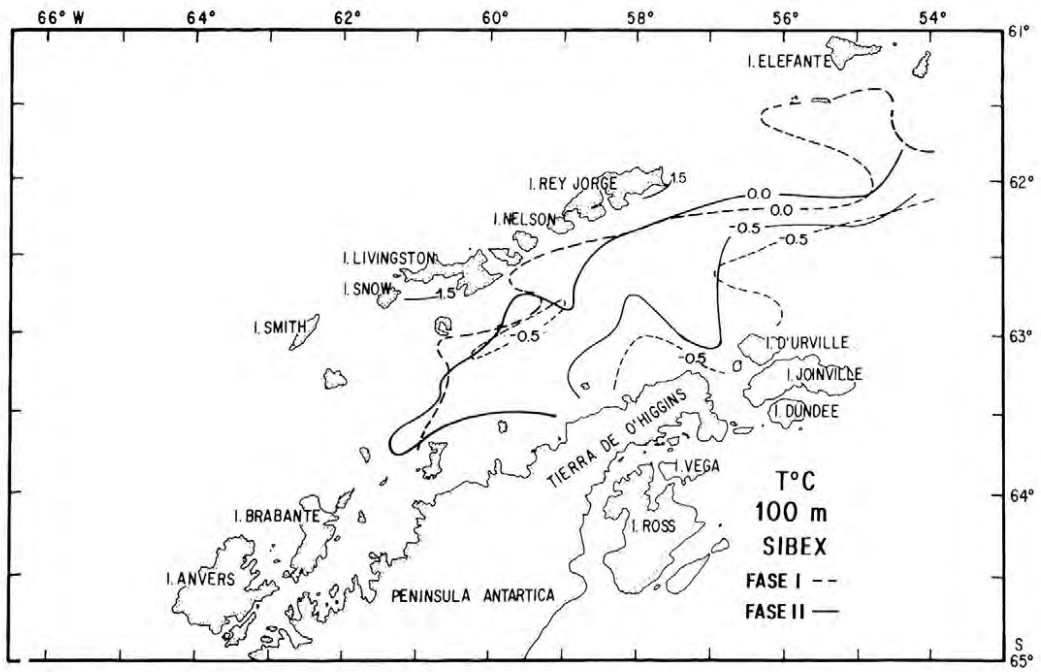


**Figure 4b.**—Position of a pair of isotherms of the SIBEX-Phase I (January 27 - February 10, 1984) and SIBEX-Phase II (January 24 - February 15, 1985) cruises, at 100 m level.

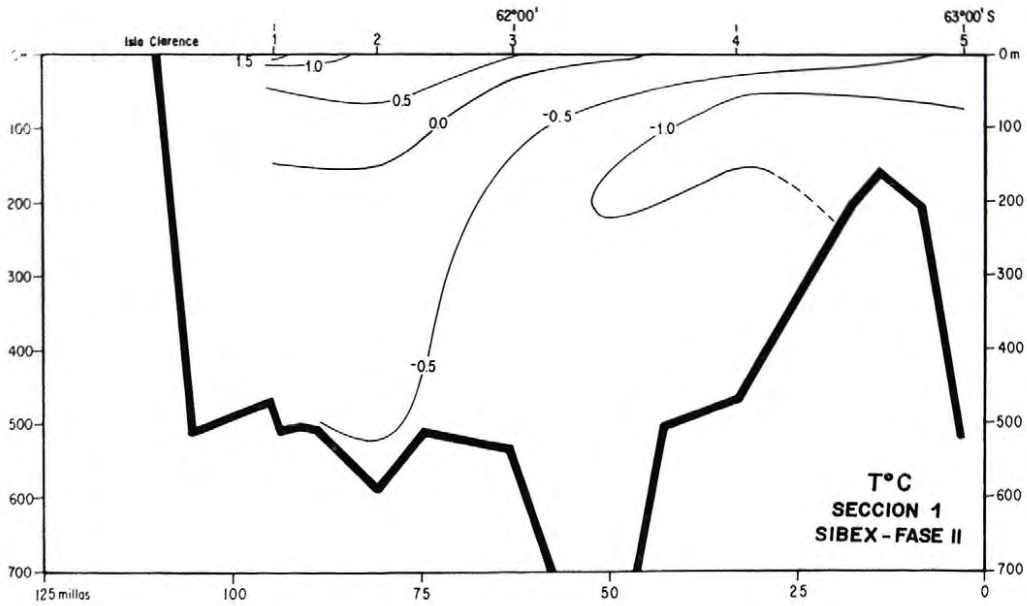


Figure 5.—Vertical distribution of temperature in Section 1.

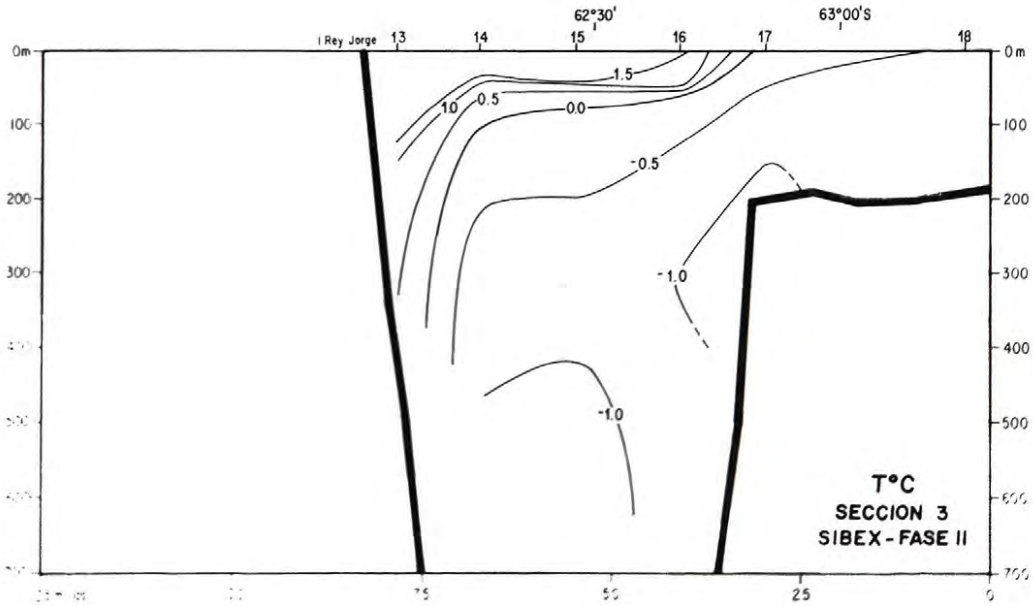


Figure 6.—Vertical distribution of temperature in Section 3.

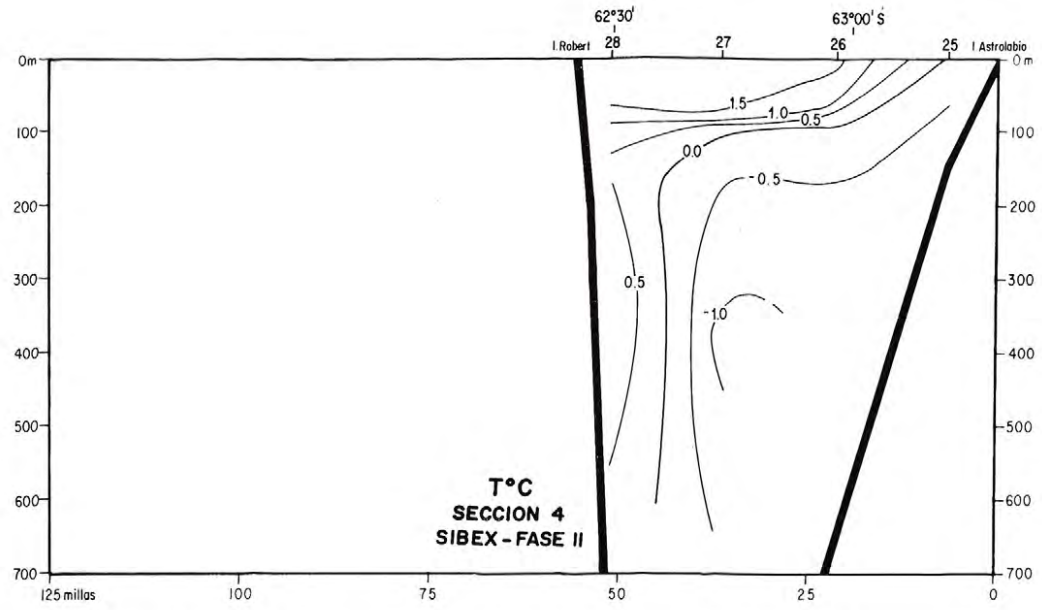


**Figure 7.**—Vertical distribution of temperature in Section 4.

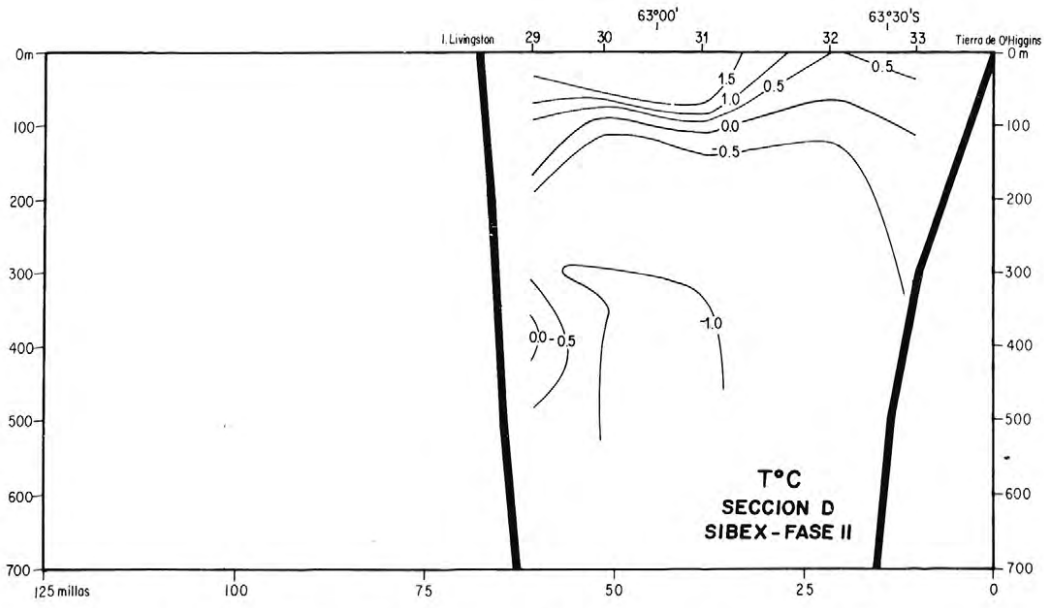


**Figure 8.**—Vertical distribution of temperature in Section D.

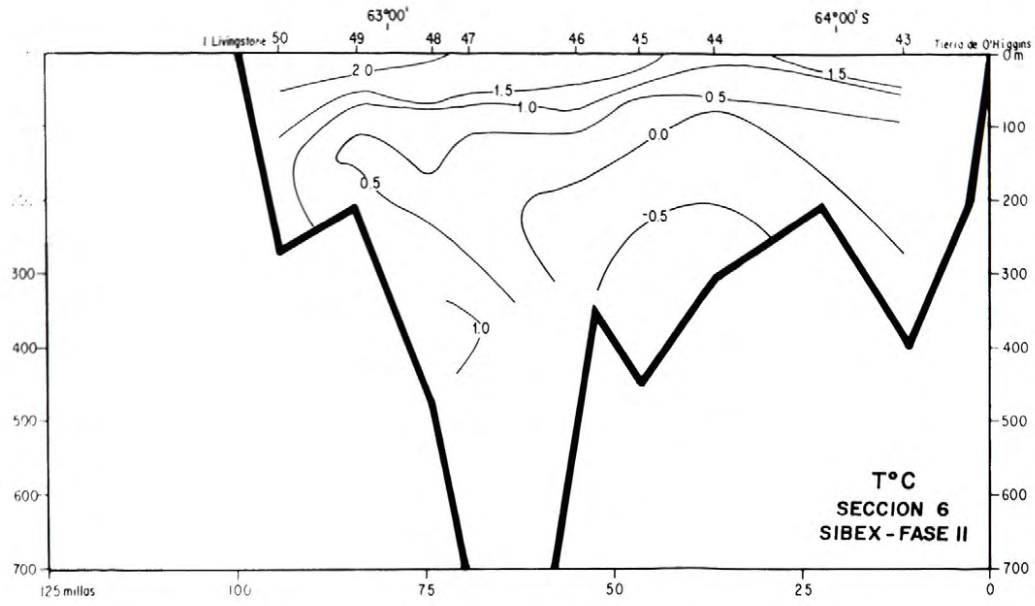


Figure 9.—Vertical distribution of temperature in Section 6.

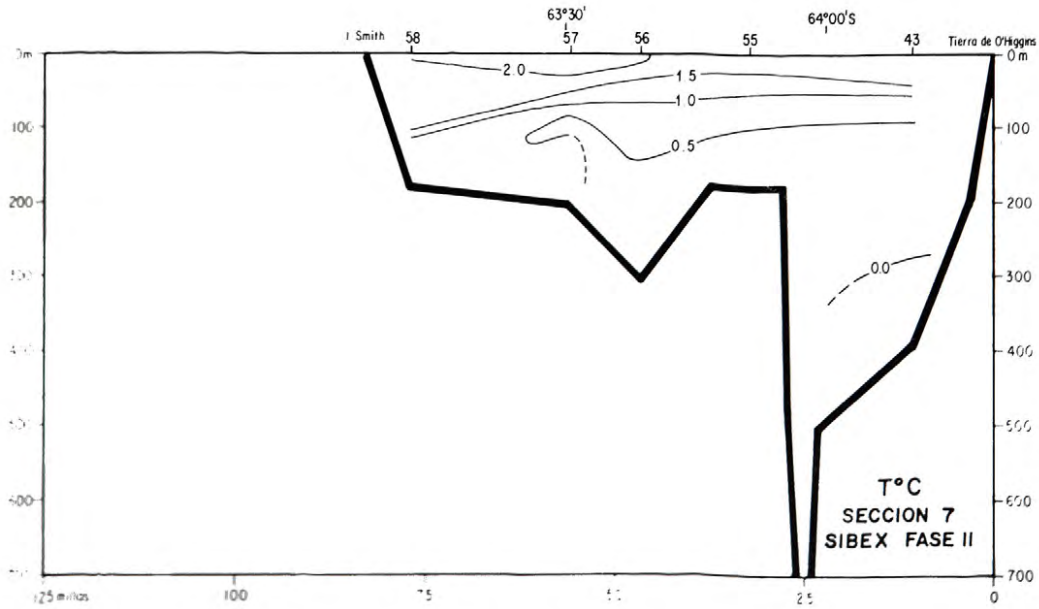


Figure 10.—Vertical distribution of temperature in Section 7.

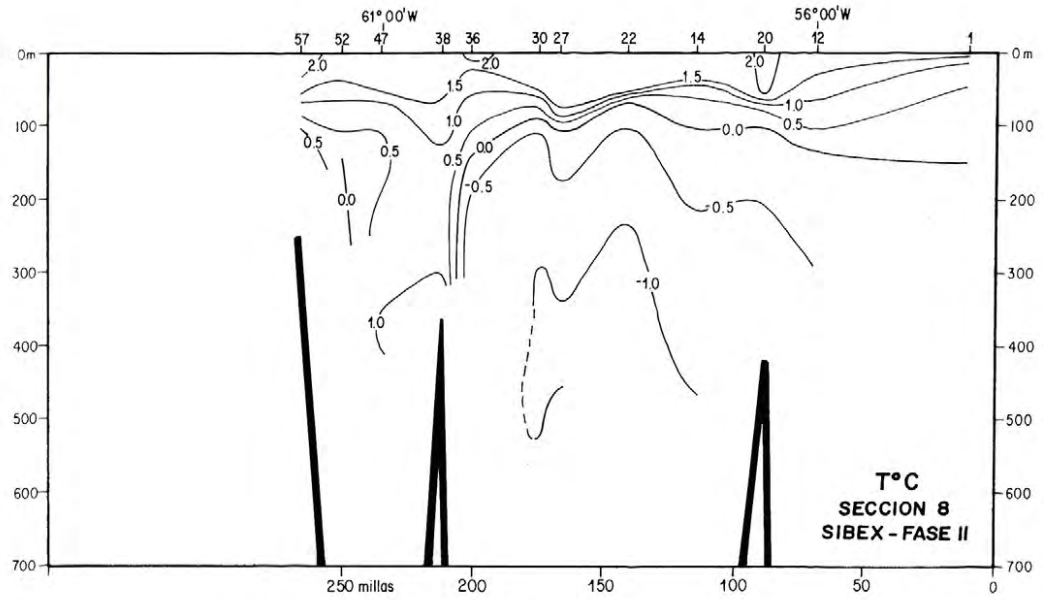


**Figure 11.**—Vertical distribution of temperature in Section 8.

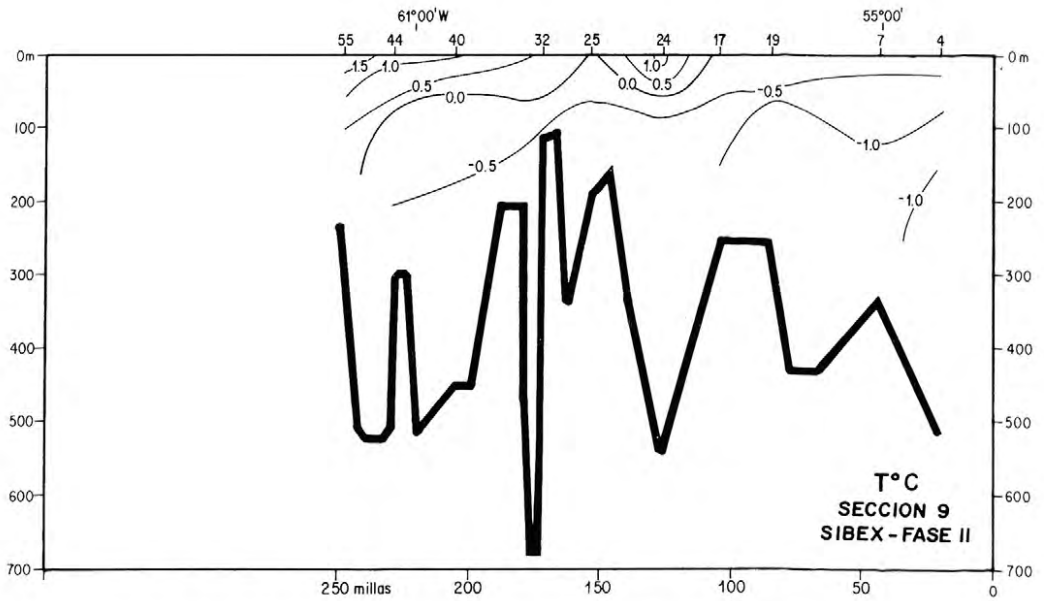


**Figure 12.**—Vertical distribution of temperature in Section 9.

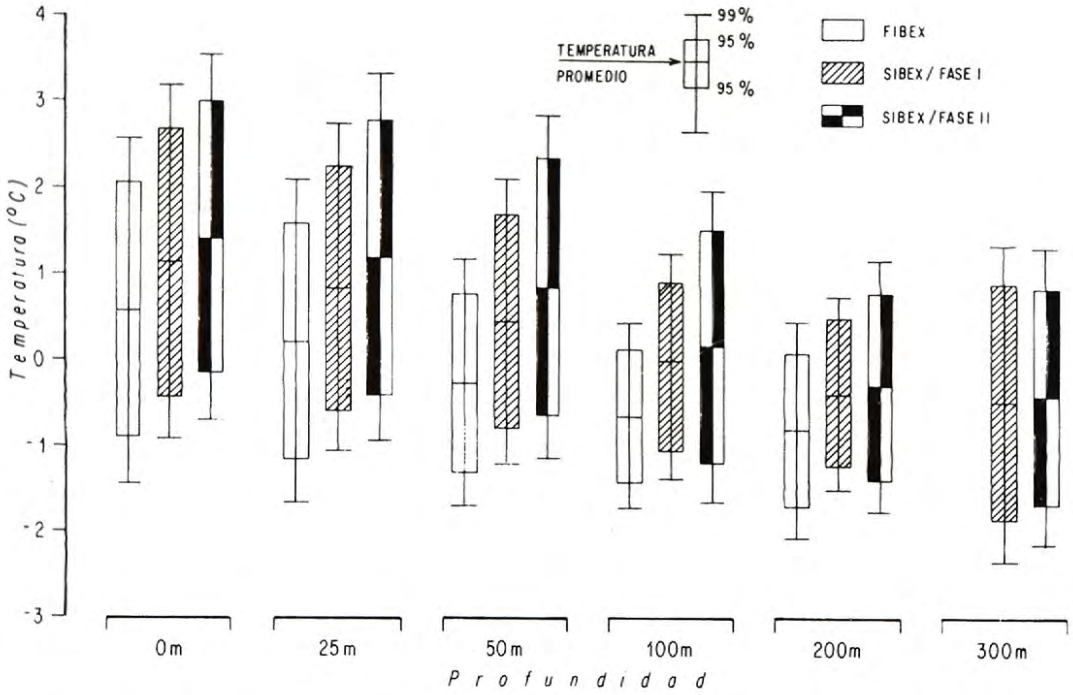


Figure 13.—Comparison of the average temperature at the following levels: 0, 25, 50, 100, 200, 300 m for a common area, during FIBEX (January - February, 1981), SIBEX-Phase I (January - February, 1984) and SIBEX-Phase II (January - February, 1985) cruises. The temperature values are included for 95% and 99% confidence level.

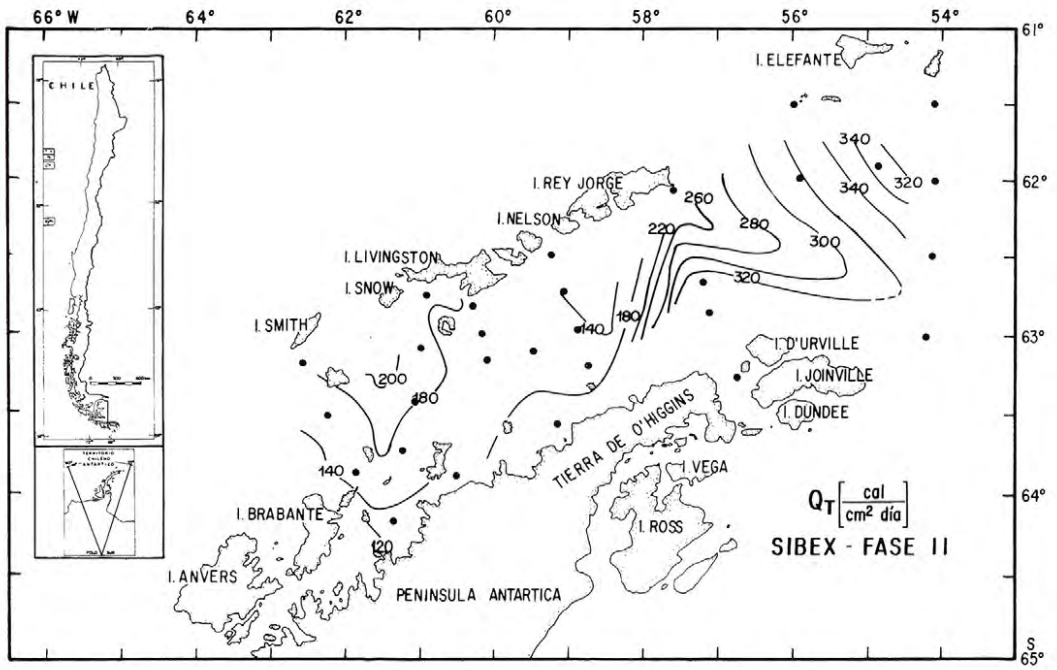


**Figure 14.**—Net flux of the atmosphere heat to the ocean in unities of cal/cm$^2$/day. The punctual instantaneous values have been averaged horizontaly in grills of 0.5° latitude and 1° longitude.

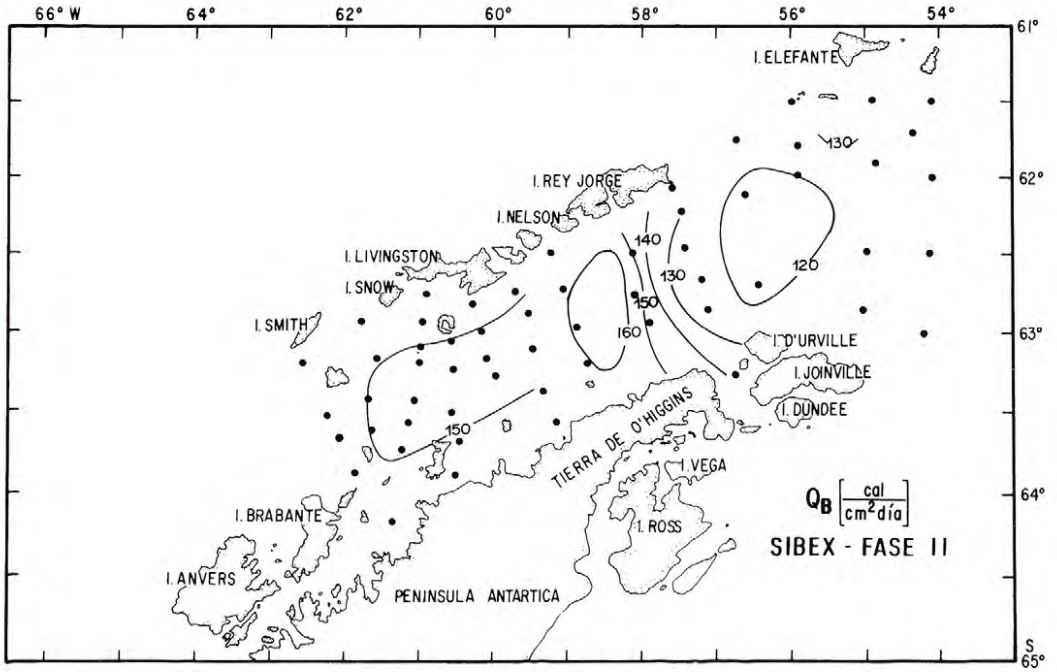


**Figure 15.**—Heat fluxe in long wave radiation delivered by the ocean to the atmosphere in units of cal/cm$^2$/day. The punctual instantaneous values have been averaged horizontaly in grills of 0.5° latitude and 1° longitude.

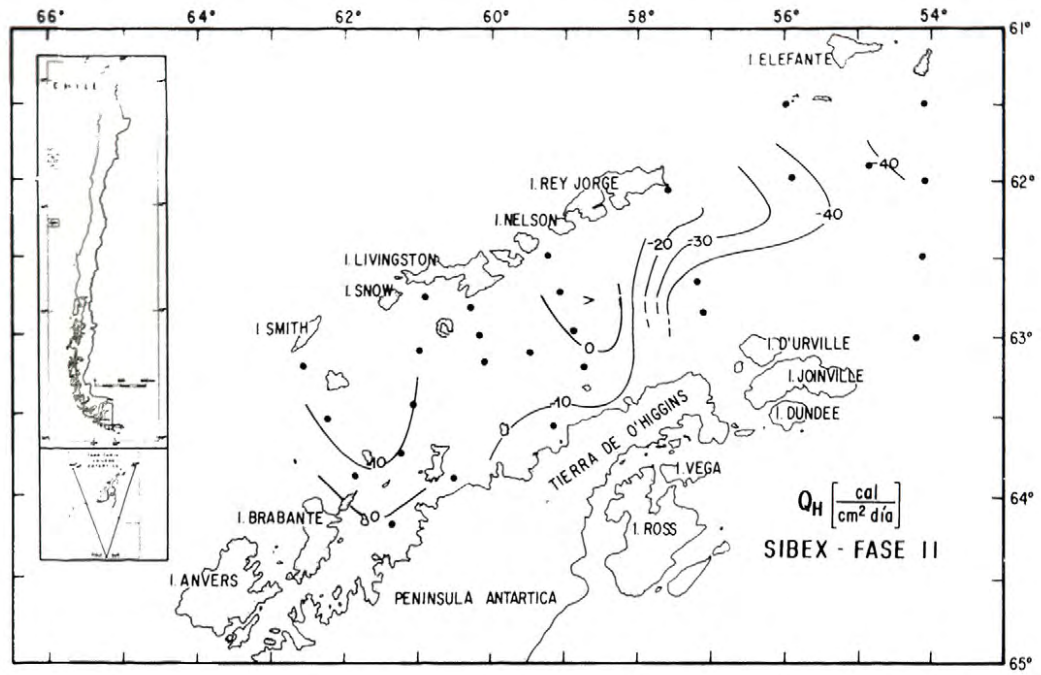


Figure 16.—Sensitive heat fluxe from the atmosphere to the ocean in cal/cm$^2$/day. The instantaneous punctual values have been averaged horizontaly in grills of 0.5° latitude and 1° longitude.

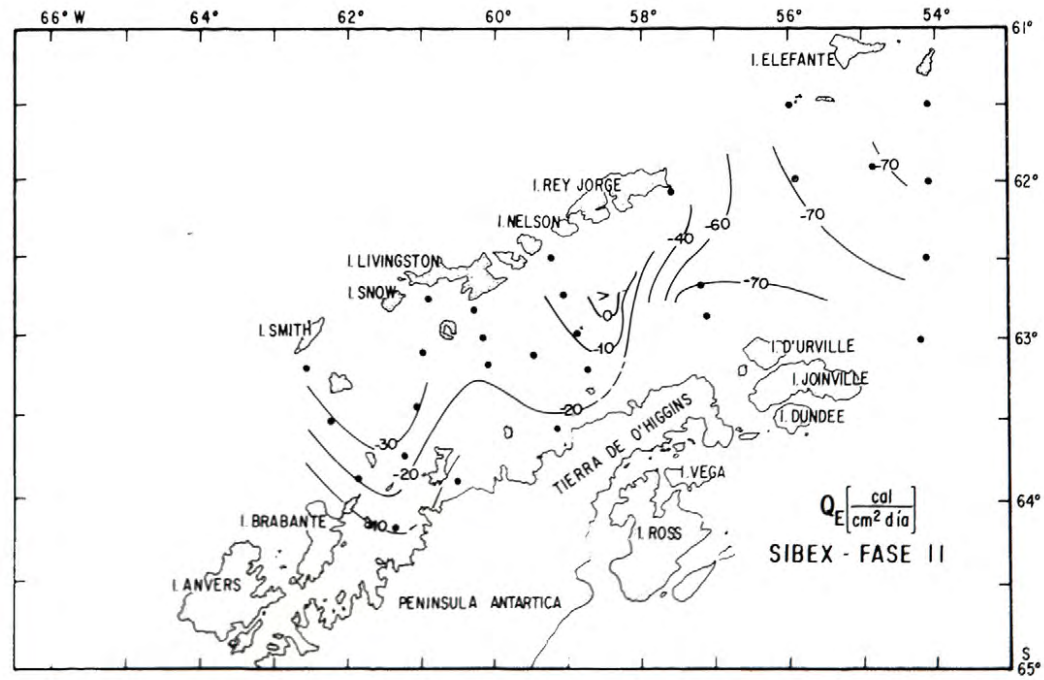


Figure 17.—Latent heat flux from the atmosphere to the ocean in units cal/cm$^2$/day. The instantaneous punctual values have been averaged in grills of 0.5° latitude and 1° longitude.

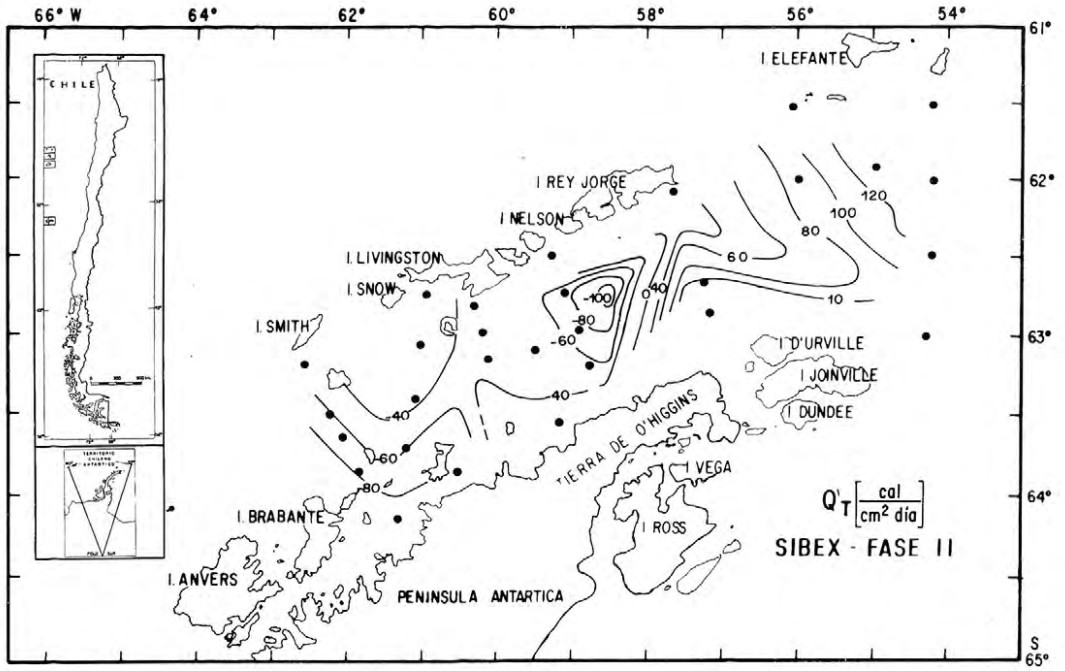


**Figure 18.**—Anomaly of atmospheric flux heat to the ocean with respect to the monthly average for the area. Units in cal/cm$^2$/day. The punctual instantaneous values have been horizontaly averaged in grills of 0.5° latitude by 1° longitude. Positive values indicate heat gain by the ocean and viceversa.

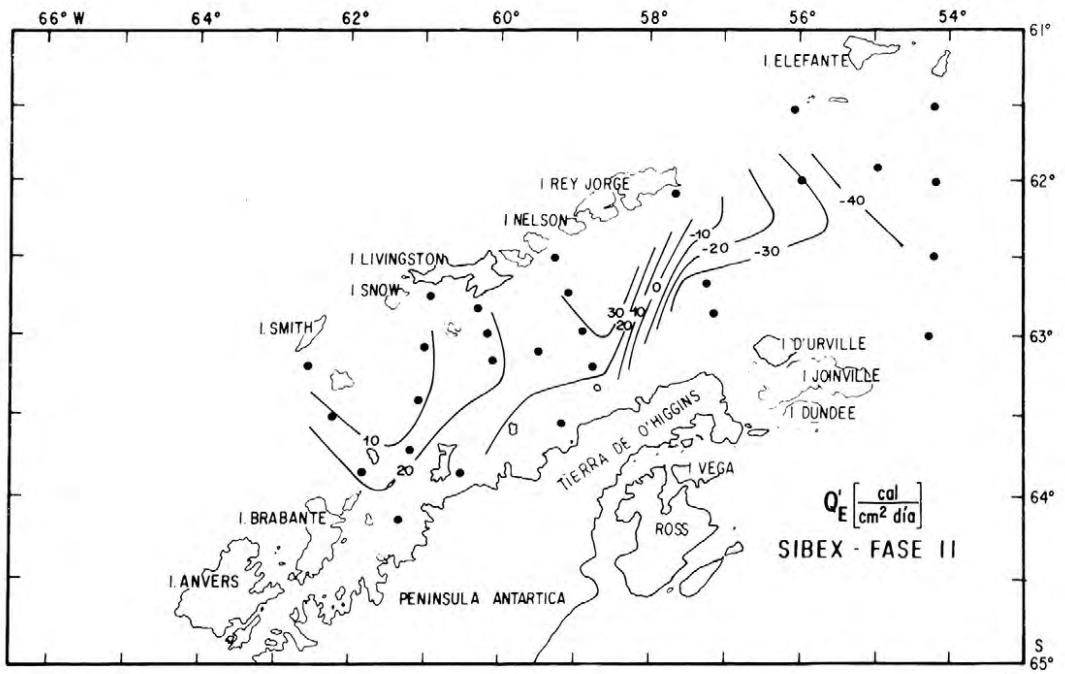


**Figure 19.**—Anomaly of atmospheric latent flux heat to the ocean with respect to the monthly average for the area. Units in cal/cm$^2$/day. The punctual instantaneous values have been horizontaly averaged in grills of 0.5° latitude by 1° longitude. Positive values show heat gains by part of the ocean and viceversa.

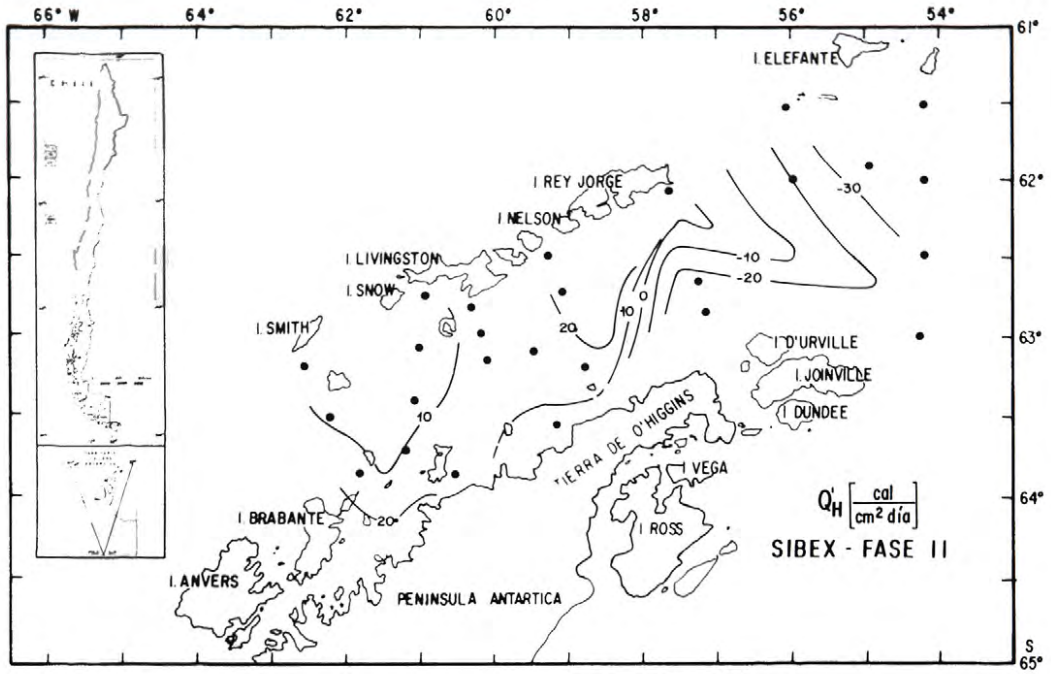


Figure 20.—Anomaly of the atmospheric sensitive heat flux to the ocean with respect to monthly average for the area. Units in cal/cm$^2$/day. The instantaneous punctual values have been horizontal averaged in grills of 0.5° latitude by 1° longitude. Positive values show heat gains by part of the ocean and viceversa.

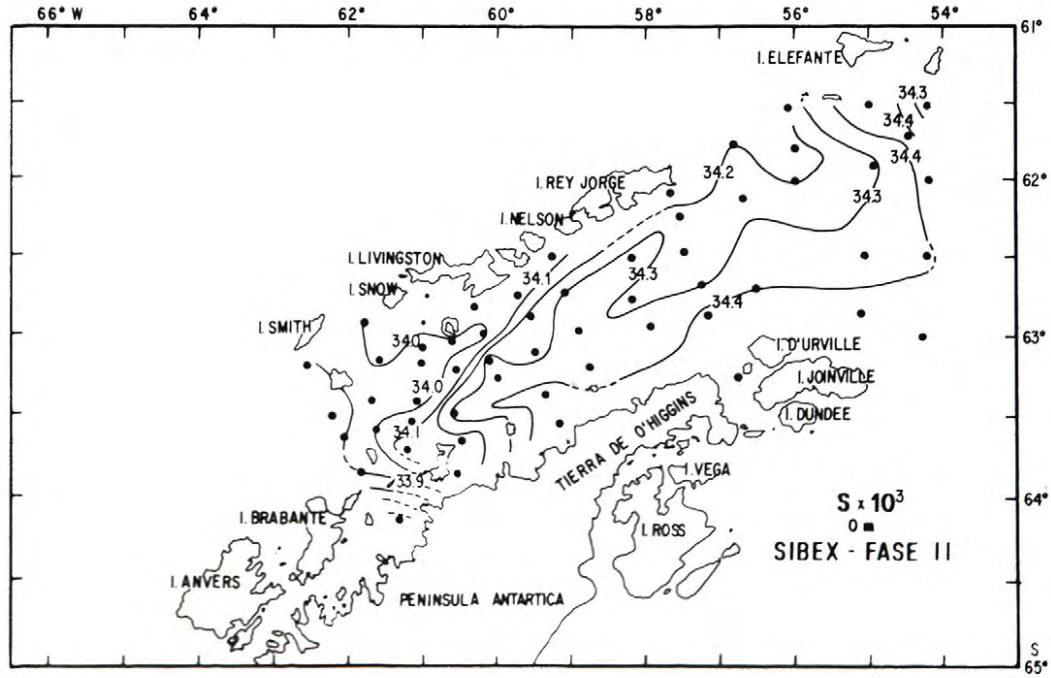


Figure 21.—Horizontal salinity distribution at 0 m level.

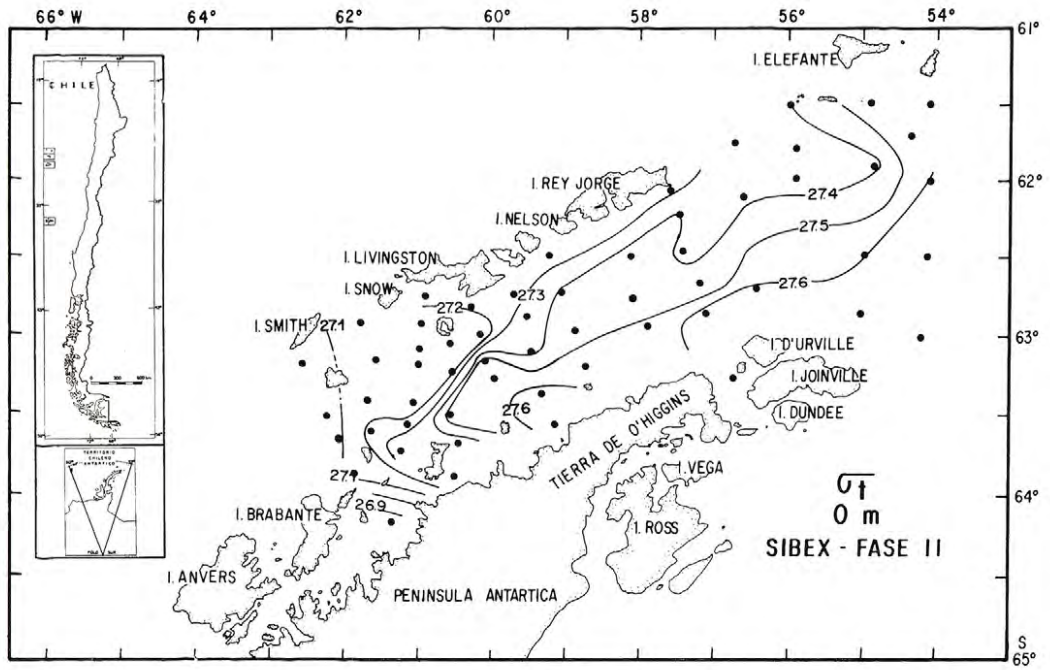


Figure 22.—Horizontal density distribution at 0 m level.

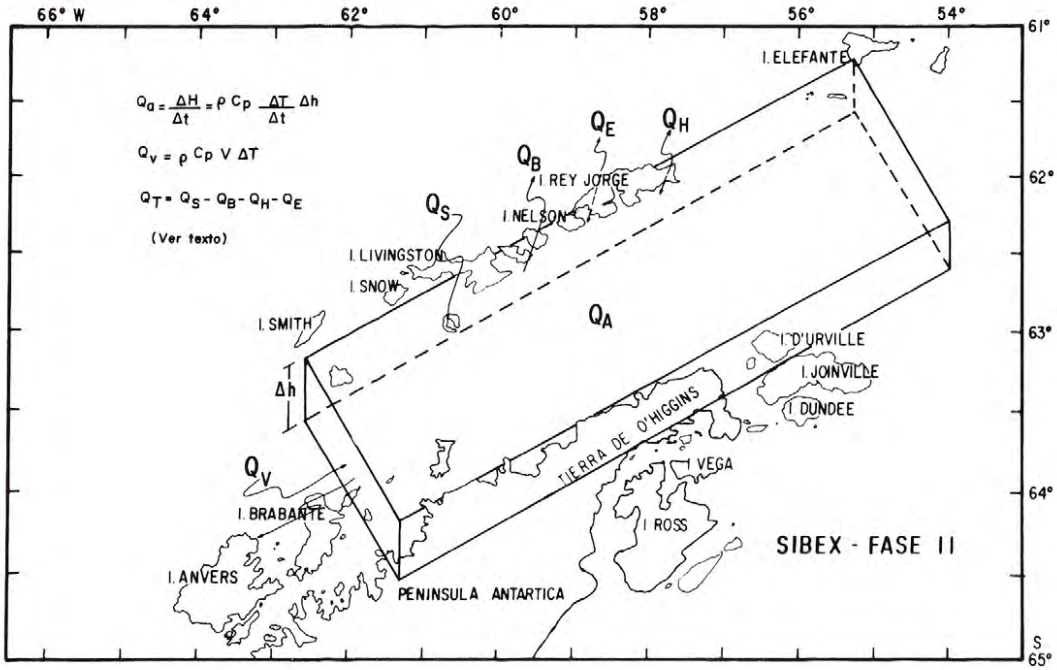


Figure 23.—Box model utilized for heat balance in the Bransfield Strait. Qa is the energy gained or lost at the box in the time Δ t; Qv is the advected heat inside or outside the box; Qt is the net interchange ocean-atmosphere. Simbology explained in the text.

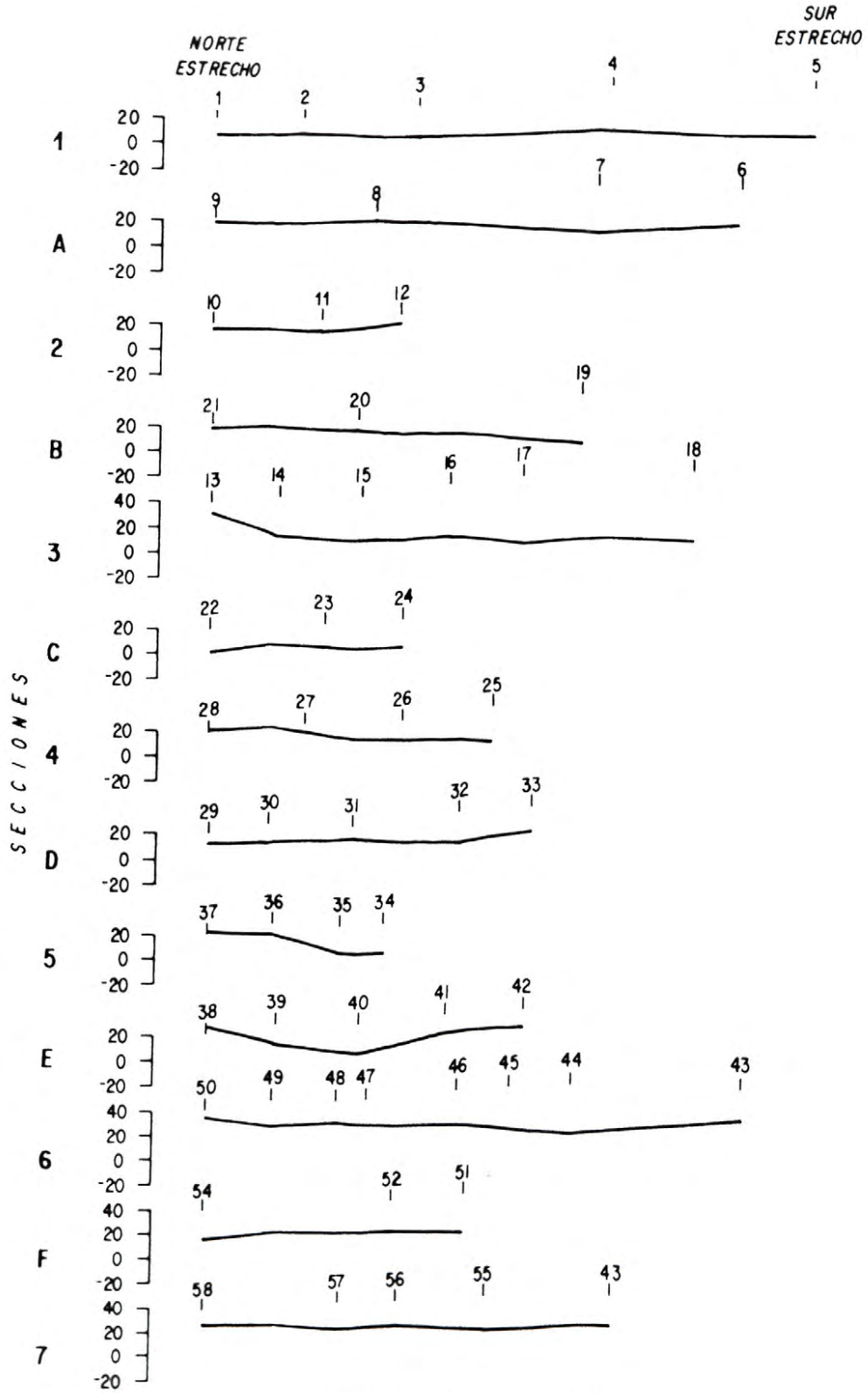


Figure 21. - Values of heat contents in Kcal/cm$^2$ in a water column between the surface and 200 m deep for each one of the north-south Sections performed during SIBEX-Phase II (January 24 - February 15, 1985). The numbers on the profiles correspond to the respective XBT number.

## REFERENCES


ANDERSON, R. J. and S. D. SMITH, 1981. Evaporations coefficient for the sea surface from eddy flux measurements. Journal of Geophysical Research, 86: 449-456.

CLOWES, A. I. J., 1934. Hidrology of the Bransfield Strait. Discovery Report, 9, 64 pags.

GORDON, A. L. and W. D. NOWLIN Jr., 1978. The basin waters of the Bransfield Strait. Journal of Physical Oceanography, 8: 258-264.

GORDON, A. L., 1981. Seasonality of Southern Ocean Sea Ice. Journal of Geophysical Research, 86: 4193-4197.

GUZMAN, O., H., BERSH, M. STEIN and R. B. HEYWOOD, 1983. Second Post-FIBEX Hydrographic Data Interpretation Workshop, Hamburg, F. R. G., 16-20 mayo 1983. BIOMASS Rep. Ser., 31: 26 pags.

KELLY, R., J. L. BLANCO y M. DIAZ, 1985. Hidrografía del estrecho Bransfield durante el verano austral 1984 (SIBEX-Fase I) Ser. Cient. INACH 33: 15-48.

LIST, R., J., 1951. Smithsonian Meteorological Tables, 6th revised edition. Smithsonian Institution Press. Washington D.C., 527 pags.

OSTLE, R. and R. W. MENSING, 1979. Statistic in Research. The Iowa State University, Ames, 596 pags.

PATTERSON, S. L. and H. A. SIEVERS, 1980. The Weddell-Scotia Confluence. Journal of Physical Oceanography, 10: 1584-1610.

ROJAS, R. L., 1985. Descripción de la estructura térmica del estrecho Bransfield a base de observaciones de XBT (SIBEX-Fase I Chile). Ser. Cient. INACH 33: 89-119.

SALAMANCA, M. A. y C. A. ACUÑA, 1982. Estudio sobre oceanografía química en las masas de agua en que habita el krill. Ser. Cient. INACH 28, 137-161.

SIEVERS, H. A., 1982. Descripción de las condiciones oceanográficas físicas, como apoyo a la distribución y comportamiento del krill, Ser. Cient. INACH 28, 87-136.

SILVA, N., 1985. Oceanografía química de las aguas del estrecho Bransfield: compuestos micronutrientes (Crucero SIBEX-1984), Ser. Cient. INACH 33, 49-87.

STEIN, M. and S. RAKUSA-SUSZCZEWSKI, 1983. Geostrophic currents in the South Shetland Islands area during FIBEX. Memoirs of National Institute of Polar Research Special Issue. 27. Proceedings of the BIOMASS Colloquium in 1982: pp. 24-34.